

# A highly selective and sensitive fluorescent turn-on sensor for Hg<sup>2+</sup> and its application in live cell imaging†

Hua Lu,<sup>a</sup> Liqin Xiong,<sup>b</sup> Hanzhuang Liu,<sup>a</sup> Mengxiao Yu,<sup>b</sup> Zhen Shen,<sup>\*a</sup> Fuyou Li<sup>\*b</sup> and Xiaozeng You<sup>\*a</sup>

Received 11th February 2009, Accepted 6th April 2009

First published as an Advance Article on the web 29th April 2009

DOI: 10.1039/b902912e

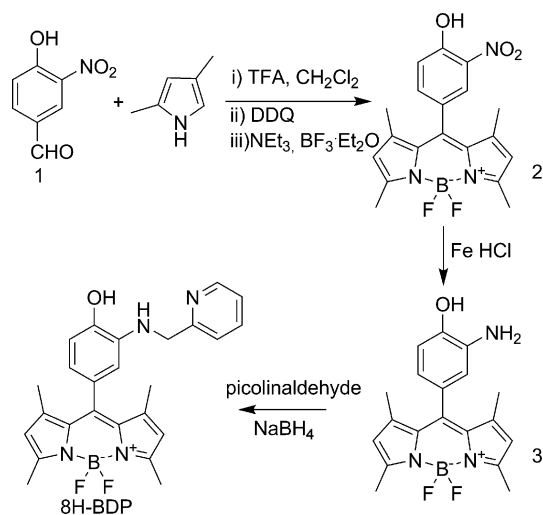
A boron–dipyrrromethene (BODIPY) derivative containing a tridentate diaza-oxa ligand (**8H-BDP**) was synthesized as a fluorescent turn-on chemosensor for Hg<sup>2+</sup> with high sensitivity (detection limit  $\leq 2$  ppb), a rapid response time ( $\leq 5$  seconds) and specific selectivity over other cations under physiological conditions and in live cells according to the confocal fluorescence microscopy experiment.

## Introduction

The concern for the worldwide spread of mercury pollution and its damage to human health and the environment has stimulated the development of efficient, selective and sensitive methods for monitoring Hg<sup>2+</sup> in environmental and biological systems.<sup>1</sup> A number of highly selective and sensitive fluorescent chemosensors have been extensively exploited for the detection of Hg<sup>2+</sup> in solution, however, only a few examples of *in vivo* monitoring of Hg<sup>2+</sup> have been reported,<sup>2</sup> including two fluorescein chemosensors bearing a thio-crown moiety,<sup>2d–2e</sup> several rhodamine-based fluorescent turn-on probes,<sup>2f–2k</sup> and a ratiometric fluorescent probe based on a BODIPY–rhodamine system.<sup>2l</sup> Several limitations such as low water solubility, poor selectivity toward other metal ions, and weak sensitivity in physiological conditions prevent the sensor molecules being applicable in biological systems. Moreover, Hg<sup>2+</sup> often causes a turn-off fluorescence response due to the heavy atom or spin-orbit coupling effect. Therefore, the exploration of new fluorescent turn-on probes for analyzing Hg<sup>2+</sup> *in vivo* with appropriate selectivity, high sensitivity, rapid response, and good water solubility remains a challenge.

Owing to their remarkable photophysical properties, such as high molar extinction coefficients (usually  $> 80\,000$  L (mol·cm)<sup>-1</sup>), high fluorescence quantum yields (commonly  $\Phi_f > 0.5$ ), excellent photostability, easy structural modification and appropriate redox potential,<sup>3</sup> recently, boron–dipyrrromethene (BODIPY) derivatives have been widely employed for detecting K<sup>+</sup>,<sup>4</sup> Cd<sup>2+</sup>,<sup>5</sup> CN<sup>-</sup>,<sup>6</sup> ClO<sup>-</sup>,<sup>7</sup> Zn<sup>2+</sup>,<sup>8</sup> and Hg<sup>2+</sup>.<sup>9</sup> However, the lipophilicity of the BODIPY moiety limited their applications in biotechnology.<sup>10</sup> Herein, we report a rational design, relying on the “receptor–spacer–fluorophore” approach,<sup>11</sup> toward the development of fluorescence sensors for Hg<sup>2+</sup> in aqueous media as well as in living cells. With a hydrophilic diaza-oxa tridentate ligand based on Hpyramol (2-*N*-(2-pyridylmethyl)amino-phenol)<sup>12</sup> as a receptor, we designed and synthesized 8-(3-*N*-(2-pyridylmethyl)amino-4-

hydroxyphenyl)-4,4-difluoro-1,3,5,7-tetramethyl-4-bora-3a,4a-diaza-*s*-indacene (**8H-BDP**) (Scheme 1) as a highly selective and sensitive fluorescence turn-on chemosensor for Hg<sup>2+</sup>. Furthermore, confocal fluorescence microscopy experiments demonstrated that **8H-BDP** could be used to monitor Hg<sup>2+</sup> in living cells.



Scheme 1 Synthetic procedures for the preparation of **8H-BDP**.

Scheme 1 outlines the synthesis of **8H-BDP**. The intermediate **2** was prepared through the TFA catalyzed condensation reaction of 3-nitro-4-hydroxybenzaldehyde with 2,4-dimethylpyrrole according to a published procedure.<sup>3a</sup> Reduction of **2** with Fe–HCl gave another compound **3**, which was reacted with picolinaldehyde to afford **8H-BDP** in 19% yield. The structure of **8H-BDP** was confirmed by <sup>1</sup>H NMR, MS spectra and single-crystal X-ray diffraction analysis.

## Results and discussion

### Structure of 8H-BDP

The molecular structure of **8H-BDP** is shown in Fig. 1. Similar to the previously reported structures of alkyl substituted BODIPYs,<sup>13</sup> the indacene plane in **8H-BDP** was nearly planar since the deviation from the mean plane was 0.0581 Å. The *meso* (or 8)-phenyl ring was virtually orthogonal to the indacene plane

<sup>a</sup>State Key Laboratory of Coordination Chemistry, Nanjing National Laboratory of Microstructures, Nanjing University, Nanjing, 210093, P.R. China. E-mail: zshen@nju.edu.cn, youxz@nju.edu.cn

<sup>b</sup>Department of Chemistry & Laboratory of Advanced Materials, Fudan University, Shanghai, 200433, P.R. China. E-mail: fyli@fudan.edu.cn

† Electronic supplementary information (ESI) available: Supplementary data, <sup>1</sup>H NMR spectra and X-ray analysis of **8H-BDP**. CCDC reference number 671844. For ESI and crystallographic data in CIF or other electronic format see DOI: 10.1039/b902912e

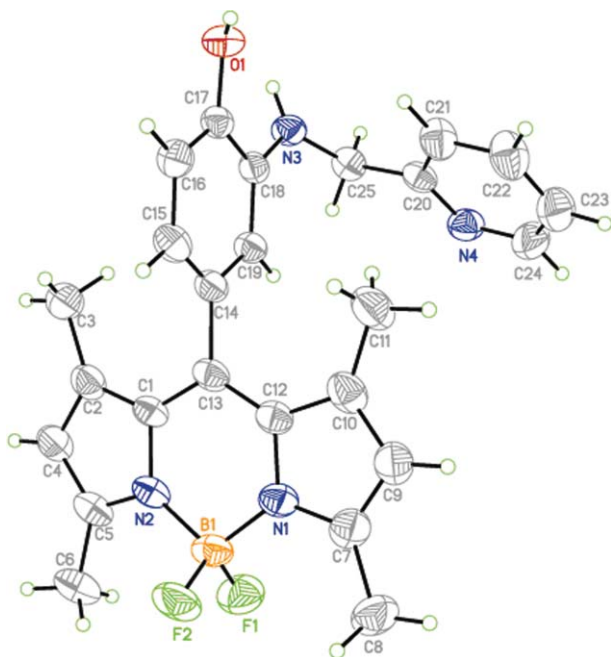


**Fig. 1** ORTEP view of the molecular structure of **8H-BDP** at 30% probability. The solvent molecule was omitted for clarity.

with the torsion angle being  $87.5^\circ$ . The pyridyl ring was tilted to the *meso*-phenyl plane with a torsion angle of  $80.2^\circ$ . The neighboring **8H-BDP** molecules were linked through intermolecular O1-H $\cdots$ N4 hydrogen bonds to form a one-dimensional chain along the *b* axis (Fig. S1, ESI $^\dagger$ ). There were no strong  $\pi$ - $\pi$  interactions within the chain.

### Hg $^{2+}$ recognition in aqueous solution

As expected, **8H-BDP** in DMSO-HEPES buffer (1 : 99, v/v, pH = 7.2) solution showed a very weak fluorescence with a quantum yield ( $\Phi_0$ ) of 0.002, which was attributed to the efficient photoinduced electron transfer (PET) quenching process from the electron-donating Hpyramol receptor to the excited BDP fluorophore.<sup>14</sup> Upon addition of Hg $^{2+}$ , the fluorescence intensity increased remarkably and a fluorescence enhancement factor at 509 nm of approximately 27-fold was estimated. Its fluorescence intensity was almost not influenced by the addition of 10 eq of Zn $^{2+}$ , Cu $^{2+}$ , Cd $^{2+}$ , Co $^{2+}$ , Fe $^{3+}$ , Mn $^{2+}$ , Ni $^{2+}$ , Mg $^{2+}$ , Na $^+$ , Al $^{3+}$ , Ca $^{2+}$ , and Fe $^{2+}$ , respectively. A small influence by the addition of 10 eq of Pb $^{2+}$  ( $I/I_0 = 2.4$ ) and 10 eq of Ag $^+$  ( $I/I_0 = 3.6$ ) was observed (Fig. 2a). To evaluate the utility of **8H-BDP** as a Hg $^{2+}$ -selective fluorescent sensor, ion interference experiments were carried out. As shown in Fig. 2b, its Hg $^{2+}$  response was not interfered in the background containing the appropriate metal ions. These facts suggested that **8H-BDP** could recognize Hg $^{2+}$  ions with high selectivity under physiological conditions.

The sensitivity of **8H-BDP** to Hg $^{2+}$  was further investigated by fluorescence spectroscopy. Upon addition of the Hg $^{2+}$  ion at different concentrations in a DMSO-HEPES buffer (1 : 99, v/v, pH = 7.2) solution, as shown in Fig. 3, the fluorescence intensity of **8H-BDP** increased gradually with a virtually unchanged peak position, typical of PET.<sup>15</sup> Interestingly, before reaching the stoichiometric point, the observed fluorescent intensity was pro-

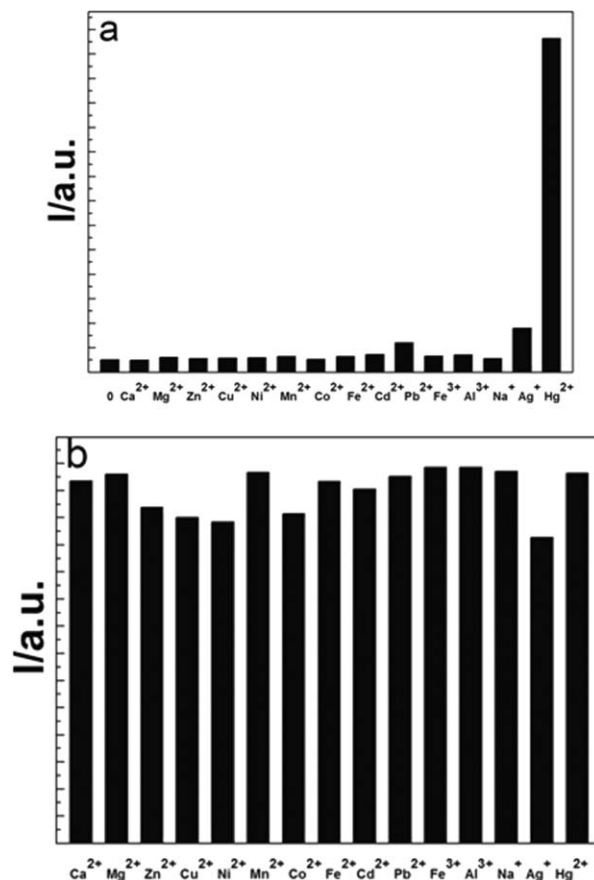


**Fig. 2** (a) Fluorescence responses of 5  $\mu\text{M}$  of **8H-BDP** upon addition of 50  $\mu\text{M}$  of different metal ions and 5  $\mu\text{M}$  of Hg $^{2+}$ . (b) Fluorescence responses of the addition of 5  $\mu\text{M}$  Hg $^{2+}$  to 5  $\mu\text{M}$  of **8H-BDP** in the presence of the appropriate metal ions (200  $\mu\text{M}$  for Mg $^{2+}$ , Na $^+$ , Ca $^{2+}$  and Zn $^{2+}$ ; 50  $\mu\text{M}$  for Cd $^{2+}$ , Co $^{2+}$ , Fe $^{3+}$ , Mn $^{2+}$ , Ni $^{2+}$ , Ag $^+$ , Al $^{3+}$ , Fe $^{2+}$  and Pb $^{2+}$ ; 5  $\mu\text{M}$  for Cu $^{2+}$ ). Spectra were acquired in a DMSO-HEPES buffer (50 mM HEPES, 50 mM KNO $_3$ , 1 : 99, v/v, pH = 7.2) solution,  $\lambda_{\text{ex}} = 470$  nm.

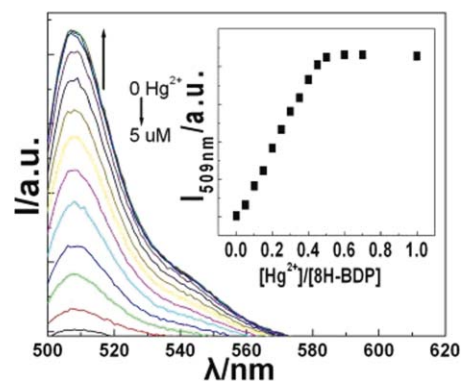


**Fig. 3** Fluorescence response of 5  $\mu\text{M}$  of **8H-BDP** upon addition of Hg $^{2+}$ . The amounts of Hg $^{2+}$  employed are 0, 0.05, 0.1, 0.15, 0.2, 0.25, 0.3, 0.35, 0.4, 0.45, 0.5, 0.6, 0.7, and 1.0 equiv., respectively. Spectra were acquired in a DMSO-HEPES buffer (50 mM HEPES, 50 mM KNO $_3$ , 1 : 99, v/v, pH = 7.2) solution.  $\lambda_{\text{ex}} = 470$  nm.

portional to the concentration of Hg $^{2+}$  ion; subsequent addition of Hg $^{2+}$  ( $>0.5$  eq.) caused an unchanged behaviour in the fluorescence intensity, indicating that the Hg $^{2+}$  sensor had a 1 : 2 stoichiometry<sup>16</sup> (Fig. 3). The association constant  $\log K_s$  was determined to be

$18.2 \pm 0.1$  from a nonlinear least-square analysis of fluorescence intensity *versus* the concentration of  $\text{Hg}^{2+}$  (Fig. S2, ESI†).

For a fluorescent molecular sensor to be practically used, the detection limit is an important factor. When **8H-BDP** was employed at  $0.5 \mu\text{M}$  in a DMSO–HEPES buffer ( $50 \text{ mM HEPES}$ ,  $50 \text{ mM KNO}_3$ ,  $1 : 999$ , v/v,  $\text{pH} = 7.2$ ) solution,  $\text{Hg}^{2+}$  could be detected at least down to  $2 \text{ ppb}$ , which is the U.S. Environmental Protection Agency's limit for drinking water.<sup>17</sup> Under these conditions, the fluorescent intensity of **8H-BDP** was nearly proportional to the concentration of  $\text{Hg}^{2+}$  added (Fig. 4). Furthermore, the interaction of **8H-BDP** with  $\text{Hg}^{2+}$  was completed in a few seconds (Fig. S3, ESI†), therefore **8H-BDP** could be used for the real-time and real-space analysis of  $\text{Hg}^{2+}$  ions in cells and organisms.

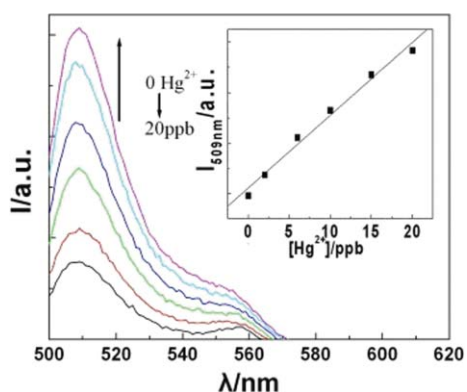


**Fig. 4** Fluorescence response of **8H-BDP** ( $0.5 \mu\text{M}$ ) to  $\text{Hg}^{2+}$  in a DMSO–HEPES buffer ( $50 \text{ mM HEPES}$ ,  $50 \text{ mM KNO}_3$ ,  $1 : 999$ , v/v,  $\text{pH} = 7.2$ ) solution.  $\lambda_{\text{ex}} = 470 \text{ nm}$ . Inset figure: titration curve of  $I_{509\text{nm}}$  vs.  $\text{Hg}^{2+}$  concentration.

### Intracellular imaging of $\text{Hg}^{2+}$

Then, we evaluated the practical applicability of **8H-BDP** as a  $\text{Hg}^{2+}$  probe to operate within living cells. Cells supplemented with  $50 \mu\text{M}$  of  $\text{HgCl}_2$  for  $1 \text{ h}$  at  $37^\circ\text{C}$  and then incubated with  $50 \mu\text{M}$  of **8H-BDP** for  $10 \text{ min}$  at  $25^\circ\text{C}$ , showed a significant fluorescence emission from the intracellular region (Fig. 5b), as determined by laser scanning confocal microscopy (using an Olympus FluoView FV1000). In the control experiment, staining HeLa cells with only  $50 \mu\text{M}$  **8H-BDP** or  $50 \mu\text{M}$   $\text{Hg}^{2+}$  under the same conditions showed weak intracellular fluorescence (Fig. 5a and Fig. S4, ESI†). The marked increase observed in intracellular fluorescence was attributed to the interaction between **8H-BDP** and  $\text{Hg}^{2+}$ . Further brightfield measurements after treatment with both  $\text{Hg}^{2+}$  and **8H-BDP** confirmed that the cells were viable throughout the imaging experiments (Fig. 5c). As shown in Fig 5d, the overlay of fluorescence and brightfield images revealed that the fluorescence signals were localized in the perinuclear region of the cytosol, which was confirmed by the high signal-to-noise ratio ( $I_2/I_1 > 200$ ) between the cytoplasm (region 2) and the background (region 1) (Fig. S5, ESI†).

In addition, large signal ratios ( $I_2/I_3 > 20$ ) between the cytoplasm (region 2) and nucleus (region 3) mean weak nuclear uptake and exclusive staining in the cytoplasm for **8H-BDP**. This was also confirmed by Z-scan luminescence imaging of HeLa cells stained with both **8H-BDP** and  $\text{Hg}^{2+}$  (Fig. 6 and Fig. S6, ESI†). The above results indicated that **8H-BDP** was

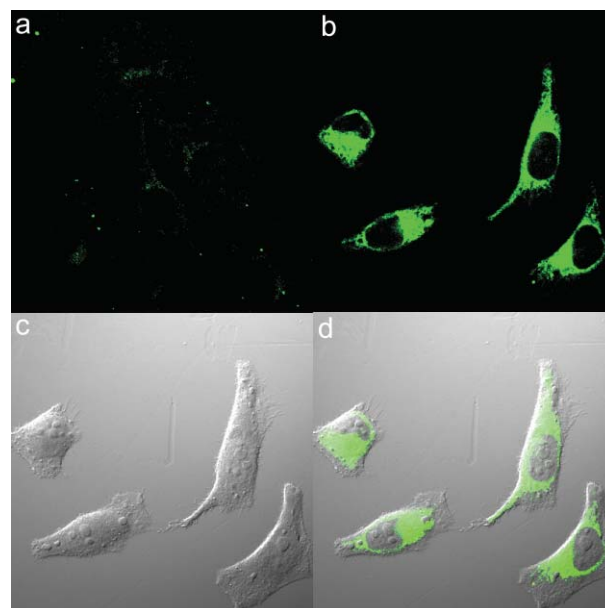


**Fig. 5** Confocal fluorescence and brightfield images of HeLa cells. (a) Cells incubated with  $50 \mu\text{M}$  of **8H-BDP** for  $10 \text{ min}$  at  $25^\circ\text{C}$ . (b) Cells supplemented with  $50 \mu\text{M}$  of  $\text{Hg}^{2+}$  in the growth media for  $1 \text{ h}$  at  $37^\circ\text{C}$  and then stained with  $50 \mu\text{M}$  of **8H-BDP** for  $10 \text{ min}$  at  $25^\circ\text{C}$ . (c) Brightfield image of cells showed in panel b. The overlay of panels b and c is shown in d ( $\lambda_{\text{ex}} = 488 \text{ nm}$ ).

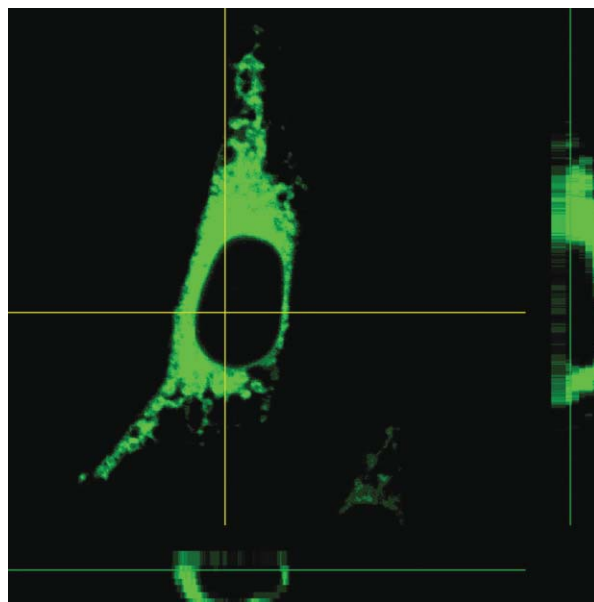


**Fig. 6** Z-scan image of the live HeLa cells supplemented with  $50 \mu\text{M}$  of  $\text{Hg}^{2+}$  in the growth media for  $1 \text{ h}$  at  $37^\circ\text{C}$  and then stained with  $50 \mu\text{M}$  of **8H-BDP** for  $10 \text{ min}$  at  $25^\circ\text{C}$ .

cell-permeable and could respond to variations in intracellular  $\text{Hg}^{2+}$ .

In summary, we have demonstrated a boron–dipyromethene (BDP) derivative **8H-BDP** with a diaza-oxa tridentate ligand of Hpyramol as a fluorescence turn-on chemosensor for  $\text{Hg}^{2+}$  in aqueous media. This chemosensor showed a very high sensitivity (detection limit  $\leq 2 \text{ ppb}$ ), a rapid response time ( $\leq 5 \text{ seconds}$ ), and high selectivity for  $\text{Hg}^{2+}$  over other metal cations. Such

significantly enhanced fluorescence of **8H-BDP** upon addition of  $\text{Hg}^{2+}$  is probably attributed to the formation of a 2 : 1 complex of **8H-BDP**– $\text{Hg}^{2+}$  in which the PET quenching process is efficiently suppressed by coordination with the  $\text{Hg}^{2+}$  ion. Moreover, confocal fluorescence microscopy experiments have established the utility of **8H-BDP** in monitoring  $\text{Hg}^{2+}$  within living cells, indicating its potential application for studying the effect of  $\text{Hg}^{2+}$  in biological systems.

## Experimental section

### Materials and methods

All reagents were obtained from commercial suppliers and used without further purification unless otherwise indicated. All air- and moisture-sensitive reactions were carried out under nitrogen atmosphere in oven-dried glassware. Dichloromethane was distilled over calcium hydride. Triethylamine was obtained by simple distillation. Elemental analyses for C, H and N were performed on a Perkin-Elmer 240C elemental analyzer. NMR spectra were recorded on a Bruker DRX500 spectrometer and referenced to the residual proton signals of the solvent. Mass spectra were measured with a Bruker Daltonics Autoflex IITM MALDI TOF spectrometer. Luminescence spectra were measured on an Edinburgh LFS-920 fluorescence spectrophotometer and an Aminco Bowman 2 Luminescence spectrophotometer. The fluorescence quantum yield was calculated using Rhodamine 6G ( $\Phi = 0.88$  in EtOH) as a reference.

Stock solutions of the metal ions (1 mM) and  $\text{Hg}^{2+}$  (10 mM, 1 mM, 0.1 mM) were prepared in deionized water. A stock solution of **8H-BDP** (0.5 mM) was prepared in DMSO. The solution of **8H-BDP** was then diluted to 5  $\mu\text{M}$  with HEPES buffer solution (1 : 99, v/v, pH 7.2). In the titration experiments, a 2 mL solution of **8H-BDP** (5  $\mu\text{M}$ , 0.5  $\mu\text{M}$ ) was poured into a quartz optical cell of 1 cm optical path length each time, and the  $\text{Hg}^{2+}$  stock solution was added into the quartz optical cell gradually by using a micro-pipette. Spectral data were recorded immediately after the addition. In selectivity experiments, the test samples were prepared by placing the appropriate amounts of metal ion stock solution into 2 mL solution of **8H-BDP** (5  $\mu\text{M}$ ). For fluorescence measurements, excitation was provided at 470 nm, and emission was collected from 500 to 580 nm.

### X-Ray structure determination

The X-ray diffraction data were collected on a Bruker Smart Apex CCD diffractometer with graphite monochromated Mo K $\alpha$  radiation ( $\lambda = 0.71073 \text{ \AA}$ ) using the  $\omega$ -2 $\theta$  scan mode. The data were corrected for Lorentz and polarization effects. The structure was solved by direct methods and refined on  $F^2$  by full-matrix least-squares methods using SHELXTL-2000. All calculations and molecular graphics were carried out on a computer using the SHELX-2000 program package and Diamond.

**8H-BDP**· $\text{CH}_3\text{OH}$ .  $\text{C}_{26}\text{H}_{29}\text{BF}_2\text{N}_4\text{O}_2$ ; a red block-like crystal of the approximate dimensions  $0.23 \times 0.21 \times 0.20 \text{ mm}^3$  was measured. Monoclinic, space group  $P2_1/c$ ,  $a = 14.6725(14) \text{ \AA}$ ,  $b = 10.8383(10) \text{ \AA}$ ,  $c = 18.7883(13) \text{ \AA}$ ,  $\beta = 127.732(5)^\circ$ ,  $V = 2363.0(4) \text{ \AA}^3$ ,  $Z = 4$ ,  $F(000) = 1008$ ,  $\rho = 1.396 \text{ Mg m}^{-3}$ ,  $2\theta_{\text{max}} =$

$56.52^\circ$ ,  $R_1 = 0.0673$ ,  $R_w = 0.1892$ ,  $\text{GOF} = 0.930$ , residual electron density between 0.883 and  $-0.685 e \text{ \AA}^{-3}$ .†

### Cell culture and fluorescence bioimaging

The HeLa cell line was provided by the Institute of Biochemistry and Cell Biology, SIBS, CAS (China). Cells were grown in MEM (modified Eagle's medium) supplemented with 10% FBS (fetal bovine serum) at 37 °C and 5%  $\text{CO}_2$ . Cells ( $5 \times 10^8$  per L) were plated on 14 mm glass coverslips and allowed to adhere for 24 h. Experiments to assess  $\text{Hg}^{2+}$  uptake were performed over 1 h in the same medium supplemented with 50  $\mu\text{M}$   $\text{Hg}(\text{ClO}_4)_2$ .

Immediately before the experiments, cells were washed with PBS buffer and then incubated with 50  $\mu\text{M}$  of **8H-BDP** in PBS for 10 min at 25 °C. Cell imaging was then carried out after washing the cells with PBS. Confocal fluorescence imaging was performed with an Olympus FV1000 laser scanning fluorescence microscope and a 60 $\times$  oil-immersion objective lens. Cells incubated with **8H-BDP** were excited at 488 nm using a multi-line argon laser. Emission was collected from 500 to 540 nm.

### Synthesis

**8-(3-Nitro-4-hydroxyphenyl)-4,4-difluoro-1,3,5,7-tetramethyl-4-bora-3a,4a-diaza-s-indacene (2)**. 2,4-Dimethylpyrrole (380 mg, 4 mmol) and 3-nitro-4-hydroxybenzaldehyde (334 mg, 2 mmol) were dissolved in dry  $\text{CH}_2\text{Cl}_2$  (150 mL) under nitrogen. One drop of trifluoroacetic acid (TFA) was added, and the solution was stirred for 4 h at ambient temperature in the dark (until TLC indicated complete consumption of the aldehyde). 2,3-Dichloro-5,6-dicyanoquinone (DDQ, 442 mg, 2 mmol) was added, and the mixture was stirred for an additional 30 min. The reaction mixture was then treated with triethylamine (3 mL) for 5 min. Boron trifluoride etherate (3 mL) was added and the mixture was stirred for another 40 min, the dark brown solution was washed with water ( $3 \times 20 \text{ mL}$ ) and brine (30 mL), dried over anhydrous magnesium sulfate, and concentrated at reduced pressure. The crude product was purified by silica-gel flash column chromatography (10% EtOAc–petroleum ether) and recrystallization from  $\text{CHCl}_3$ –hexane yielded **2** as red crystals (150 mg, yield 19%). Mp  $> 200^\circ\text{C}$ . IR (KBr pellet,  $\text{cm}^{-1}$ ): 3447, 2924, 1634, 1548, 1512, 1465, 1415, 1382, 1311, 1192, 1156, 1088, 937.  $\lambda_{\text{max}}$  ( $\text{CHCl}_3$ )/nm 479 ( $\epsilon/\text{dm}^3 \text{ mol}^{-1} \text{ cm}^{-1}$  14 800) and 507 (61 700).  $^1\text{H NMR}$  (500 MHz,  $\text{CDCl}_3$ ) 10.73 (s, 1 H), 8.13 (s, 1 H), 7.55 (d, 1 H,  $J = 5 \text{ Hz}$ ), 7.36 (d, 1 H,  $J = 8.5 \text{ Hz}$ ), 6.05 (s, 2 H), 2.59 (s, 6 H), 1.49 (s, 6 H). MS (MALDI-TOF):  $m/z$  385.210  $[\text{M}]^+$ . Anal. Calcd for  $\text{C}_{19}\text{H}_{18}\text{BF}_2\text{N}_3\text{O}_3$ ; C, 59.25; H, 4.71; N, 10.91; found C, 59.38; H, 4.63; N, 10.93%.

**8-(3-Amino-4-hydroxyphenyl)-4,4-difluoro-1,3,5,7-tetramethyl-4-bora-3a,4a-diaza-s-indacene (3)**. Compound **2** (150 mg, 0.39 mmol) was dissolved in 5 mL of methanol.  $\text{H}_2\text{O}$  (3 mL) and Fe (300 mg, 5.4 mmol) were added and the reaction mixture was heated to reflux. Hydrochloric acid in a methanol solution (2 mL, 0.6 mol  $\text{L}^{-1}$ ) was added dropwise. The solution was refluxed for 2 h until TLC monitoring indicated complete consumption of the starting material. After cooling to room temperature, filtration and concentration at reduced pressure, the crude product was purified by silica-gel flash column chromatography (20% EtOAc–petroleum ether) and recrystallization from  $\text{CHCl}_3$ –hexane yielded **3** as red crystals (105 mg, yield 75%). Mp  $> 200^\circ\text{C}$ . IR (KBr pellet,

cm<sup>-1</sup>): 3430, 2923, 1620, 1544, 1507, 1469, 1406, 1382, 1302, 1197, 1158, 1085, 983.  $\lambda_{\text{max}}$  (CHCl<sub>3</sub>)/nm 474 ( $\epsilon/\text{dm}^3 \text{ mol}^{-1} \text{ cm}^{-1}$  12 900) and 502 (56 700). <sup>1</sup>H NMR (500 MHz, CDCl<sub>3</sub>) 6.84 (d, 1 H, *J* = 9 Hz), 6.66 (s, 1 H), 6.56 (d, 1 H, *J* = 7.5 Hz), 5.99 (s, 2 H), 2.56 (s, 6 H), 1.54 (s, 6 H). MS (MALDI-TOF): *m/z* 355.148 [M]<sup>+</sup>, 336.157 [M – F]<sup>+</sup>. Anal. Calcd for C<sub>19</sub>H<sub>20</sub>BF<sub>2</sub>N<sub>3</sub>O; C, 64.25; H, 5.68; N, 11.83; found C, 64.43; H, 5.62; N, 11.72%.

### 8-(3-*N*-(2-Pyridylmethyl)amino-4-hydroxyphenyl)-4,4-difluoro-1,3,5,7-tetramethyl-4-bora-3 $\alpha$ ,4 $\alpha$ -diazas-indacene (8H-BDP).

Compound **3** (105 mg, 0.3 mmol), picolinaldehyde (32 mg, 0.3 mmol) and one drop of acetic acid in MeOH (10 mL) were refluxed for 24 h. After cooling to room temperature, NaBH<sub>4</sub> (30 mg, 0.8 mmol) was slowly added and the reaction mixture was refluxed continuously for another 12 h. After removing the volatiles under reduced pressure, water (20 mL) was added to the resulting residue. The pH value of the mixture was adjusted to ca. 7 by adding glacial acetic acid, and the mixture was extracted with EtOAc (3  $\times$  15 mL), dried over anhydrous magnesium sulfate, and concentrated at reduced pressure. The crude product was purified by silica-gel flash column chromatography (40% EtOAc–petroleum ether) and recrystallization from CH<sub>3</sub>OH–hexane yielded **8H-BDP** as red crystals (25 mg, yield 18.7%). Mp >200 °C. IR (KBr pellet, cm<sup>-1</sup>): 3428, 2924, 1601, 1546, 1510, 1470, 1407, 1384, 1307, 1197, 1157, 1085, 978.  $\lambda_{\text{max}}$  (CH<sub>3</sub>OH)/nm 469 ( $\epsilon/\text{dm}^3 \text{ mol}^{-1} \text{ cm}^{-1}$  13 500) and 507 (52 100). <sup>1</sup>H NMR (500 MHz, CD<sub>3</sub>OD) 8.39 (d, 1 H, *J* = 4.5 Hz), 7.70 (m, 1 H), 7.43 (d, 1 H, *J* = 6 Hz), 7.21 (m, 1 H), 6.79 (d, 1 H, *J* = 9 Hz), 6.33 (d, 1 H, *J* = 9 Hz), 6.24 (s, 1 H), 5.93 (s, 2 H), 5.46 (s, 2 H), 4.44 (s, 2 H), 2.40 (s, 6 H), 1.33 (s, 6 H). MS (MALDI-TOF): *m/z* 446.387 [M]<sup>+</sup>, 427.399 [M – F]<sup>+</sup>. Anal. Calcd for C<sub>23</sub>H<sub>25</sub>BF<sub>2</sub>N<sub>4</sub>O; C, 67.28; H, 5.65; N, 12.55; found C, 67.15; H, 5.51; N, 12.38.

### Acknowledgements

We are thankful for financial support from the National Basic Research Program of China (Nos. 2006CB806104 and 2007CB925103), NSFC (Nos. 20875043 and 20775017), and the Shanghai Leading Academic Discipline Project (B108).

### Notes and references

- (a) E. M. Nolan and S. J. Lippard, *Chem. Rev.*, 2008, **108**, 3443; (b) D. W. Domaille, E. L. Que and C. J. Chang, *Nat. Chem. Biol.*, 2008, **4**, 168.

- (a) Z. Zhang, X. Guo, X. Qian, Z. Lu and F. Liu, *Kidney Int.*, 2004, **66**, 2279; (b) Z. Zhang, D. Wu, X. Guo, X. Qian, Z. Lu, Q. Xu, Y. Yang, L. Duan, Y. He and Z. Feng, *Chem. Res. Toxicol.*, 2005, **18**, 1814; (c) B. Tang, L. J. Cui, K. H. Xu, L. L. Tong, G. W. Yang and L. G. An, *ChemBioChem*, 2008, **9**, 1159; (d) S. Yoon, A. E. Albers, A. P. Wong and C. J. Chang, *J. Am. Chem. Soc.*, 2005, **127**, 16030; (e) S. Yoon, E. W. Miller, Q. W. He, P. H. Do and C. J. Chang, *Angew. Chem., Int. Ed.*, 2007, **46**, 6658; (f) H. Yang, Z. G. Zhou, W. W. Huang, M. Yu, F. Y. Li, T. Yi and C. H. Huang, *Org. Lett.*, 2007, **9**, 4729; (g) M. Suresh, A. Shrivastav, S. Mishra, E. Suresh and A. Das, *Org. Lett.*, 2008, **10**, 3013; (h) S. K. Ko, Y. K. Yang, J. Tae and I. Shin, *J. Am. Chem. Soc.*, 2006, **128**, 14150; (i) W. Liu, L. Xu, H. Zhang, J. You, X. Zhang, R. Sheng, H. Li, S. Wu and P. Wang, *Org. Biomol. Chem.*, 2009, **7**, 660; (j) X. Chen, S. W. Nam, M. J. Jou, Y. Kim, S. J. Kim, S. Park and J. Yoon, *Org. Lett.*, 2008, **10**, 5235; (k) Y. K. Yang, S. K. Ko, I. Shin and J. Tae, *Nature Protocols*, 2007, **2**, 1740; (l) X. Zhang, Y. Xiao and X. Qian, *Angew. Chem., Int. Ed.*, 2008, **47**, 8025.
- (a) Z. Shen, H. Röhr, K. Rurack, H. Uno, M. Spieles, B. Schulz, G. Reck and N. Ono, *Chem.–Eur. J.*, 2004, **10**, 4853; (b) Y. H. Yu, A. B. Descalzo, Z. Shen, H. Röhr, Q. Liu, Y. W. Wang, M. Spieles, Y. Z. Li, K. Rurack and X. Z. You, *Chem. Asian J.*, 2006, **1–2**, 176; (c) G. Ulrich, R. Ziessel and A. Harriman, *Angew. Chem., Int. Ed.*, 2008, **47**, 1184.
- W. Namkung, P. Padmawar, A. D. Mills and A. S. Verkman, *J. Am. Chem. Soc.*, 2008, **130**, 7794.
- T. Cheng, Y. Xu, S. Zhang, W. Zhu, X. Qian and L. Duan, *J. Am. Chem. Soc.*, 2008, **130**, 16160.
- (a) Z. Ekmekci, M. D. Yilmaz and E. U. Akkaya, *Org. Lett.*, 2008, **10**, 461; (b) J. O. Huh, Y. Do and M. H. Lee, *Organometallics*, 2008, **27**, 1022.
- Z. Sun, F. Liu, Y. Chen, P. Tam and D. Yang, *Org. Lett.*, 2008, **10**, 2171.
- S. Atilgan, T. Ozdemir and E. U. Akkaya, *Org. Lett.*, 2008, **10**, 4065.
- M. Yuan, W. Zhou, X. Liu, M. Zhu, J. Li, X. Yin, H. Zheng, Z. Zuo, C. Ouyang, H. Liu, Y. Li and D. Zhu, *J. Org. Chem.*, 2008, **73**, 5008.
- A. Loudet and K. Burgess, *Chem. Rev.*, 2007, **107**, 4891.
- K. Rurack and U. Resch-Genger, *Chem. Soc. Rev.*, 2002, **31**, 116.
- (a) Y. L. Wong, K. P. Ng and H. K. Lee, *Inorg. Chem.*, 2002, **41**, 5276; (b) Y. L. Wong, J. F. Ma, F. Xue, T. Mak and K. P. Ng, *Organometallics*, 1999, **18**, 5075; (c) L. D. Pachon, A. Golobic, B. Kozlevar, P. Gamez, H. Kooijman, A. L. Spek and J. Reedijk, *Inorg. Chim. Acta*, 2004, **357**, 3697; (d) P. U. Maheswari, S. Barends, S. Oezalp-Yaman, P. de Hoog, H. Casellas, S. J. Teat, C. Massera, M. Lutz, A. L. Spek, G. P. van Wezel, P. Gamez and J. Reedijk, *Chem.–Eur. J.*, 2007, **13**, 5213.
- Y. H. Yu, Z. Shen, H. Y. Xu, Y. W. Wang, T. Okujima, N. Ono, Y. Z. Li and X. Z. You, *J. Mol. Struct.*, 2007, **827**, 130.
- Y. Gabe, Y. Urano, K. Kikuchi, H. Kojima and T. Nagano, *J. Am. Chem. Soc.*, 2004, **126**, 3357.
- J. Bricks, A. Kovalchuk, C. Trieflinger, M. Nofz, M. Büschel, A. I. Tolmachev, J. Daub and K. Rurack, *J. Am. Chem. Soc.*, 2005, **127**, 13522.
- Y. K. Yang, K. J. Yook and J. Tae, *J. Am. Chem. Soc.*, 2005, **127**, 16760.
- Mercury Update: Impact on Fish Advisories*, EPA Fact Sheet EPA-823-F-01-011; EPA, Office of Water, Washington, DC, 2001.